GOLPH3 inhibition overcomes cisplatin resistance by restoring the glutathione/reactive oxygen species balance in the A549 non-small cell lung cancer cell line

QIONGYING WEI[1,2*], JINQUAN LIN[3,4*], ZHUANGBIN LIN[5], NANDING YU[1,2], YINGXIAO WU[1,2], XUEXUE TAN[1,2] and DAN XUE[1,2]

[1]Department of Pulmonary and Critical Care Medicine, Fujian Medical University Union Hospital, Fuzhou, Fujian 350001, P.R. China; [2]Department of Geriatrics, Fujian Medical University Union Hospital, Fuzhou, Fujian 350001, P.R. China; [3]Department of Trauma Center and Emergency Surgery, The First Affiliated Hospital, Fujian Medical University, Fuzhou, Fujian 350005, P.R. China; [4]Department of Trauma Center and Emergency Surgery, National Regional Medical Center, Binhai Campus of The First Affiliated Hospital, Fujian Medical University, Fuzhou, Fujian 350212, P.R. China; [5]Department of Radiation Oncology, Fujian Medical University Union Hospital, Fuzhou, Fujian 350001, P.R. China

Received January 27, 2024; Accepted July 17, 2024

DOI: 10.3892/or.2024.8829

Abstract. Cisplatin resistance is common in non-small cell lung cancer (NSCLC); however, the molecular mechanisms remain unclear. The present study aimed to identify a new function of Golgi phosphoprotein 3 (GOLPH3) in NSCLC-associated cisplatin resistance. Using A549 human NSCLC cells and the cisplatin-resistant variant, stable cell lines with GOLPH3 knockdown or overexpression were established using lentiviral vectors. Through Cell Counting Kit-8 and EdU assays, it was revealed that knockdown of GOLPH3 significantly enhanced cisplatin sensitivity in NSCLC cells. Specifically, flow cytometric analysis showed that GOLPH3 knockdown promoted apoptosis and G_2-phase cell cycle arrest in A549 cells. Mechanistically, intracellular reactive oxygen species (ROS) and glutathione (GSH) levels were measured using assay kits, and it was demonstrated that GOLPH3 knockdown decreased intracellular GSH levels, and further attenuated intracellular cisplatin efflux and GSH/ROS imbalance. In addition, tumor-sphere formation assays verified that GOLPH3 knockdown mitigated the stem cell-like phenotype of NSCLC cells. In conclusion, the present findings indicated the relevance of GOLPH3 in NSCLC-associated cisplatin resistance, and thus targeting GOLPH3 may be developed into a combination therapy to overcome cisplatin resistance.

Correspondence to: Professor Dan Xue, Department of Pulmonary and Critical Care Medicine, Fujian Medical University Union Hospital, 29 Xinquan Road, Fuzhou, Fujian 350001, P.R. China
E-mail: xuedan@fjmu.edu.cn

*Contributed equally

Key words: non-small cell lung cancer, cisplatin resistance, Golgi phosphoprotein 3, intracellular glutathione, reactive oxygen species

Introduction

Lung cancer is the leading cause of cancer-related death, and was estimated to be responsible for >120,000 deaths in the United States in 2023 (1). Despite improvements in early detection and treatment leading to a decline in lung cancer mortality rates, the 5-year relative survival rate remains low, particularly in non-small cell lung cancer (NSCLC) which accounts for ~82% of all reported lung cancer cases (1,2). Due to the frequently asymptomatic onset of NSCLC, most patients are diagnosed at an advanced stage, during which only 21% of patients are suitable for surgical resection, and most (61%) are treated with chemotherapy, radiation and/or immunotherapy (3,4). However, radiotherapy is not suitable for postoperative patients due to its severe side effects and deleterious effects on survival (5,6). Due to primary and acquired resistance to immunotherapy, most patients with NSCLC treated with immunotherapy do not achieve durable clinical responses (7,8). By contrast, chemotherapy exhibits a greater benefit than immunotherapy for patients with NSCLC; however, synergistic immunotherapy is also recommended as the standard of care in most patients with advanced NSCLC (9,10).

Cisplatin, an adjuvant chemotherapeutic drug that binds to DNA and induces cell death, has been recommended as a first-line drug for postoperative patients with NSCLC (11). In addition, cisplatin combined with immunotherapy has been approved for patients with inoperable advanced NSCLC (12). A pooled analysis of adjuvant cisplatin in lung cancer confirmed that cisplatin-based adjuvant chemotherapy exhibited a disease-free survival benefit of 5.8% and an overall survival benefit of 5.4%, compared with in patients who did not receive cisplatin-based adjuvant chemotherapy (13). However, most patients with NSCLC exhibit intrinsic or acquired cisplatin resistance (14,15), thus leading to ineffective responses. Therefore, there is an urgent need to understand the molecular mechanisms underlying spontaneous and acquired resistance to cisplatin.

Golgi phosphoprotein 3 (GOLPH3) is a Golgi oncoprotein that is upregulated in numerous tumors, including lung, breast and prostate cancer, and melanoma (16). High levels of GOLPH3 have been shown to be positively associated with poor survival, partly via GOLPH3-associated mTOR and WNT signaling pathway activation, which can mediate pro-tumorigenic and drug-resistant effects in patients with cancer (17). In line with this, high levels of GOLPH3 can promote the resistance to multiple chemotherapeutic drugs, such as oxaliplatin (18), 5-fluorouracil (19) and sorafenib (20). However, to the best of our knowledge, GOLPH3-mediated cisplatin resistance and the underlying mechanisms in patients with NSCLC have not been clarified. The present study aimed to investigate the role of GOLPH3 in cisplatin resistance in human NSCLC cells, and to understand the mechanisms by which GOLPH3 regulates chemotherapeutic resistance and promotes tumor metastasis.

Materials and methods

Cell culture. The A549 human NSCLC cell line was purchased from The Cell Bank of Type Culture Collection of The Chinese Academy of Sciences. A549-cisplatin resistant (A549-Cis) cells were obtained from Otwo Biotech (Shenzhen) Inc., and were created by screening cells after long-term treatment with 5 μg/ml cisplatin. Therefore, the present study also used a cisplatin concentration of 5 μg/ml. The A549 cells were cultured in RPMI 1640 medium (HyClone; Cytiva) supplemented with 10% fetal bovine serum (Gibco; Thermo Fisher Scientific, Inc.), 100 U/ml penicillin and 100 μg/ml streptomycin. The cells were maintained in a humidified incubator containing 5% CO_2 at 37˚C. The A549 cells used in the present experiments were passaged a maximum of 50 times.

Establishment of cell lines with stable expression. GOLPH3 short hairpin (sh)RNAs (shGOLPH3) and GOLPH3 overexpression (GOLPH3-OE) plasmid vectors were designed and obtained from VectorBuilder GmbH. Notably, pLV[shRNA]-EGFP:T2A:Puro-U6 was used as the vector backbone for knockdown and pLV[Exp]-EGFP:T2A:Puro-EF1A was used as the vector backbone for overexpression. Briefly, 1x10^6/dish 293T cells (The Cell Bank of Type Culture Collection of The Chinese Academy of Sciences) were plated on 10-cm dishes to clone the lentiviruses encoding shGOLPH3, noncoding negative control (NC) shRNA (shNC), GOLPH3-OE or GOLPH3-NC (empty vector). The lentiviral vectors were produced using a 3rd generation system. For each transfection, 10 μg lentiviral plasmid was used along with a 3:2:1 ratio of lentiviral vector to packaging plasmids (psPAX2) and envelope plasmids (pMD2.G). The cells were transfected at 37˚C for 48 h using Lipofectamine® 3000 (Invitrogen; Thermo Fisher Scientific, Inc.). Lentiviral particles were collected 48 h post-transfection, concentrated by ultracentrifugation and stored at -80˚C. For stable expression, A549 cells were infected with the lentiviruses encoding shGOLPH3, shNC, GOLPH3-OE and GOLPH3-NC at a multiplicity of infection of 10 at 37˚C for 24 h, followed by selection with 2 μg/ml puromycin (cat. no. P8230; Beijing Solarbio Science & Technology Co., Ltd.) at 37˚C for 72 h. GOLPH3 expression levels were verified by reverse transcription-quantitative PCR (RT-qPCR) and western blotting. The oligonucleotide sequences for shRNAs were as follows: sh1, 5'-GCTTGTGGAATGAGACGTAAACTCGAGTTTACGTCTCATTCCACAAGC-3' (target sequence: GCTTGTGGAATGAGACGTAAA); sh2, 5'-GCTTGCTTCAATCATGGTTATCTCGAGATAACCATGATTGAAGCAAGC-3' (target sequence: GCTTGCTTCAATCATGGTTAT); shNC, 5'-CCTAAGGTTAAGTCGCCCTCGCTCGAGCGAGGGCGACTTAACCTTAGG-3' (target sequence: CCTAAGGTTAAGTCGCCCTCG; this sequence has no corresponding target was found in both humans and mice). Cells were allowed to recover for 72 h post-transduction before any subsequent experimentation.

RNA isolation and RT-qPCR. Total RNA was isolated from NSCLC cells using a PureLink™ RNA isolation kit (cat. no. 12183018A; Invitrogen; Thermo Fisher Scientific, Inc.). cDNA was generated from the RNA using a PrimeScipt™ RT reagent kit (cat. no. RR037A; Takara Biotechnology Co., Ltd.) according to the manufacturer's protocol. RT was performed at 37˚C for 15 min, followed by 85˚C for 5 sec to inactivate the reverse transcriptase. qPCR was performed using SYBR Green (Bio-Rad Laboratories, Inc.) on the CFX96 touch real-time PCR system (iQ5; Bio-Rad Laboratories, Inc.). The thermocycling conditions were as follows: Initial denaturation at 95˚C for 3 min, followed by 40 cycles at 95˚C for 10 sec and 60˚C for 30 sec. β-actin was used as a normalization control and relative mRNA expression levels were calculated using the $2^{-\Delta\Delta Cq}$ method (21). The primer sequences for qPCR were as follows (5'-3'): GOLPH3, forward GATGCTCCAACAGGGGATGT, reverse TGGTGAGGGGATGTGTTGTC; ATP7A forward GCCAGCCTCTGACACAAGAA, reverse GCTCCTCTCAACGTTTCTGGA; ABCG2, forward TGGCTGTCATGGCTTCAGTA, reverse GCCACGTGATTCTTCCACAA; MATE1, forward CTTCAGGCAGGACCCAGAT, reverse CAGATAGTTGGCGAGGGCAT; MATE2K, forward ATCCTAGCCACCAGGCACTA, reverse GTGTCCACCTGCACTAGACC; ALDH1A1, forward TGGACCAGTGCAGCAAATCA, reverse ACGCCATAGCAATTCACCCA; C-myc, forward TACTGCGACGAGGAGGAGAA, reverse CGAAGGGAGAAGGGTGTGAC; β-actin, forward AACTGGGACGACATGGAGAAAA, reverse, GGATAGCACAGCCTGGATAGCA.

Western blot analysis. Total proteins were extracted from NSCLC cells with RIPA buffer (Roche Diagnostics). The protein concentration was determined using the bicinchoninic acid (BCA) assay (Pierce BCA Protein Assay Kit; Thermo Fisher Scientific, Inc.). Equal amounts of protein (30 μg/lane) were separated by SDS-PAGE on a 10% polyacrylamide gel and were transferred to polyvinylidene fluoride (PVDF) membranes (Bio-Rad Laboratories, Inc.). After blocking in 5% BSA at room temperature for 1 h, the PVDF membranes were probed with primary anti-GOLPH3 (1:1,000; cat. no. A13121; ABclonal Biotech Co., Ltd.) and anti-GAPDH (1:5,000; cat. no. AC026; ABclonal) antibodies overnight at 4˚C. Subsequently, the membranes were incubated with horseradish peroxidase-linked secondary antibodies (1:5,000; cat. no. A6154; Sigma-Aldrich; Merck KGaA) at room temperature for 1 h. The ECL Kit (Wanleibio Co., Ltd.) was used for detecting protein bands, and protein levels were semi-quantified with Image Lab software (Bio-Rad Laboratories, Inc.), normalized to GAPDH levels.

Cell viability assay. Cell viability was evaluated using the Cell Counting Kit-8 (CCK-8) assay (Dojindo Laboratories, Inc.). Briefly, 0.5-1x10^4 cells/well of NSCLC cells (infected with shNC, sh1, sh2, GOLPH3-OE and GOLPH3-NC) were seeded in 96-well plates. After an overnight incubation, the cells were treated with various concentrations of cisplatin (0, 1, 2.5, 5, 10, 25 and 50 μg/ml; Shanghai Aladdin Biochemical Technology Co., Ltd.) at 37˚C for 24 h. Subsequently, CCK-8 solution was added to the phenol red- and serum-free cell medium for another 1 h. Light absorbance at 450 nm was then recorded using an Infinite M200 Pro microplate reader (Tecan Group, Ltd.). Each concentration was tested at least three times.

EdU assay. A total of 5x10^4 cells/well of NSCLC cells (infected with shNC, sh1, sh2, GOLPH3-OE and GOLPH3-NC) were seeded in 24-well plates. After overnight incubation, the cells were treated with 5 μg/ml cisplatin at 37˚C for 24 h. Subsequently, the cells were cultured with EdU reagent (1:1,000 dilution; Beyotime Institute of Biotechnology) for another 2 h, and were fixed with 4% paraformaldehyde at 37˚C for 15 min, followed by staining with DAPI (1 μg/ml) at 37˚C for 10 min. All cells were detected using fluorescence microscopy (Leica Microsystems, Inc.).

Cell death assay. Cell death was evaluated using an Annexin V-FITC/propidium iodide (PI) Staining Kit (cat. no. CA001; Signalway Antibody LLC). Stably transduced NSCLC cells were plated onto 24-well plates at a density of 5x10^4 cells/well. After incubation for 24 h, the cells were treated with 5 μg/ml cisplatin at 37˚C for 24 h. Subsequently, the cells were washed with phosphate-buffered saline (PBS), digested with EDTA-free trypsin, resuspended in 500 μl binding buffer, and stained with 10 μl Annexin V-FITC and 10 μl PI at 37˚C for 15 min in the dark. After washing twice with PBS, the cells were immediately analyzed by flow cytometry (FACSCelesta; BD Biosciences) and fluorescence microscopy (Leica Microsystems, Inc.), the results were analyzed using FlowJo-V10-CL software (FlowJo LLC).

Cell cycle assay. Cell cycle progression was examined using a Cell Cycle Analysis Kit (cat. no. C1052; Beyotime Institute of Biotechnology). Stably transduced NSCLC cells were plated onto 24-well plates at a density of 5x10^4 cells/well and were incubated for 24 h, after which, the cells were treated with 5 μg/ml cisplatin at 37˚C for 24 h. After washing twice with PBS to remove excess cisplatin, the cells were fixed with 75% ethanol for 24 h at 4˚C, were washed twice with PBS and were treated with RNAse (100 μg/ml) and PI (50 μg/ml) solution at 37˚C for 30 min in the dark. After washing twice with PBS, the cells were assessed using flow cytometry (FACSCelesta; BD Biosciences) and the results were analyzed using FlowJo-V10-CL software.

Intracellular cisplatin concentration detection. NSCLC cells were plated onto 24-well plates at a density of 5x10^4 cells/well and were incubated at 37˚C for 24 h. The cells were treated with 5 μg/ml cisplatin-Cy5 (Xi'an Qiyue Biotechnology Co., Ltd.) at 37˚C for 24 h, and, after washing twice with PBS, intracellular cisplatin-Cy5 concentration was assessed under a fluorescence microscope (Leica Microsystems, Inc.).

Intracellular GSH detection. Intracellular GSH levels were detected using a GSH Assay Kit (cat. no. S0053; Beyotime Institute of Biotechnology). NSCLC cells were plated onto 24-well plates at a density of 5x10^4 cells/well and were incubated at 37˚C for 24 h. The cells were treated with 5 μg/ml cisplatin at 37˚C for 24 h, after which, intracellular GSH levels were measured according to the kit instructions.

Intracellular reactive oxygen species (ROS) detection. Intracellular ROS were detected using a Reactive Oxygen Species Assay Kit (cat. no. S0033S; Beyotime Institute of Biotechnology). NSCLC cells were plated onto 24-well plates at a density of 5x10^4 cells/well and were incubated for 24 h. The cells were treated with 5 μg/ml cisplatin at 37˚C for 24 h, and, after washing twice with PBS, the DCFH-DA probe was added to the culture medium and co-incubated 37˚C for another 2 h. After washing twice with PBS to remove excess DCFH-DA, the cells were resuspended in PBS and were detected using fluorescence microscopy (Leica Microsystems, Inc.).

Sphere formation assay. NSCLC cells were seeded into ultra-low cluster 6-well microplates at a density of 500 cells/well and were cultured in serum-free medium (containing 20 ng/ml basic fibroblast growth factor and epidermal growth factor, 5 μg/ml insulin, and 0.4% BSA; Dalian Meilun Biology Technology Co., Ltd.) supplemented with 5 μg/ml cisplatin. Cells were cultured for ~10 days before 3D tumor spheres (tight, spherical, nonadherent masses >50 μm in diameter) were observed and images were captured under a phase-contrast fluorescence microscope (Leica Microsystems, Inc.).

Statistical analysis. Data are presented as the mean ± SD (n=3). The experimental data were statistically analyzed by one-way analysis of variance using GraphPad Prism 7.0 statistical software (Dotmatics). For post hoc comparisons, the Fisher's least significant difference method was used, or the Tukey honestly significant difference method was used when >3 groups were compared. $P<0.05$ was considered to indicate a statistically significant difference.

Results

GOLPH3 knockdown is associated with cisplatin sensitivity. To evaluate the effects of GOLPH3 on cisplatin resistance, knockdown and overexpression of GOLPH3 using lentiviruses encoding shGOLPH3 or GOLPH3-OE was performed. The protein and mRNA expression levels of GOLPH3 were increased in GOLPH3-OE cells, and were decreased in shGOLPH3 cells (Figs. 1A and S1). Subsequently, the inhibitory effects of cisplatin on the viability of these cells were assessed. As shown in Fig. 1B, GOLPH3 knockdown significantly increased the inhibitory effects of 5 μg/ml cisplatin on cell viability by ~2 fold. By contrast, 2.5 μg/ml cisplatin reduced cell viability by ~25% in GOLPH3-knockdown cells, but had minimal impact on control cells. Moreover, the inhibitory effect of cisplatin on A549-Cis cells was significantly lower than that on A549 cells (Fig. S2). By contrast, overexpression of GOLPH3 resulted in minimal impact on the inhibitory effects of cisplatin on cell viability (Fig. 1C), indicating that GOLPH3 overexpression does not affect cisplatin resistance.

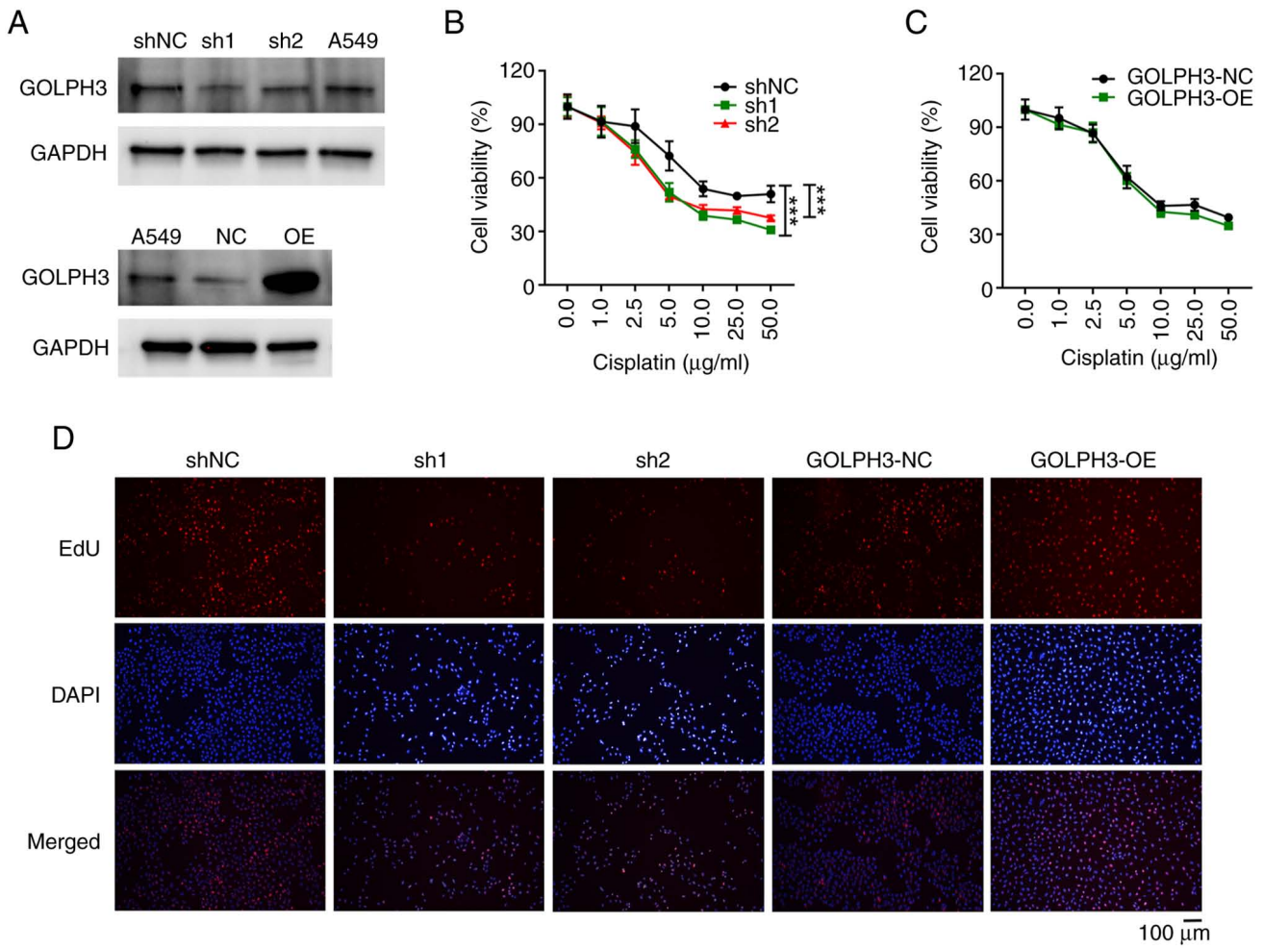

Figure 1. GOLPH3 knockdown inhibits the viability and proliferation of A549 cells. (A) GOLPH3 knockdown or OE was examined by western blot analysis. Following treatment with the indicated concentrations of cisplatin for 24 h, the viability of A549 cells infected with (B) GOLPH3 shNC, sh1 and sh2, or (C) GOLPH3-NC and GOLPH3-OE was evaluted by Cell Counting Kit-8 assay. Cell viability was suppressed in sh1 and sh2 cells, but no difference was detected in GOLPH3-OE cells. Data are presented as the mean ± SD (n=3). ***P<0.001. (D) Proliferation of A549 cells infected with GOLPH3 shNC, sh1, sh2, GOLPH3-NC and GOLPH3-OE treated with 5 μg/ml cisplatin for 24 h were examined by EdU assay. Cell proliferation was suppressed in sh1 and sh2 cells, but increased in GOLPH3-OE cells. GOLPH3, Golgi phosphoprotein 3; NC, negative control; OE, overexpression; sh, short hairpin.

Since EdU is commonly used to detect cell proliferation, cells with GOLPH3 overexpression or knockdown were treated with EdU in the presence of 5 μg/ml cisplatin. Consistent with the cell viability assay, the numbers of EdU-positive cells were markedly decreased in the GOLPH3 knockdown groups compared with those in the control group (Fig. 1D). By contrast, the numbers of EdU-positive cells were comparatively higher in the GOLPH3 overexpression group than in the control group. These findings indicated that GOLPH3 knockdown may increase cisplatin sensitivity in NSCLC cells.

The present study further investigated whether GOLPH3 knockdown could enhance the apoptosis of cells in the presence of 5 μg/ml cisplatin. A low proportion of apoptotic cells was observed in the control group, whereas the proportion was increased to 10-15% in the GOLPH3 knockdown groups (Fig. 2A and B). Consistent with the results of flow cytometry, immunofluorescence analysis showed that GOLPH3 knockdown markedly increased the proportion of Annexin V^+ and/or PI^+ cells (Fig. 2C). Moreover, cisplatin-mediated DNA toxicity was elevated in cells with GOLPH3 knockdown. As shown in Fig. 2D, GOLPH3 knockdown in A549 cells resulted in the prolongation of cisplatin-mediated cell cycle arrest at G_2 phase compared with that in the shNC group. Without cisplatin treatment, the cell cycle distribution was consistent for all cells (Fig. S3). By contrast, GOLPH3 overexpression partially abrogated cisplatin-mediated cell cycle block at G_2 phase compared with that in the GOLPH3-NC group (Fig. 2E), suggesting that GOLPH3 may impair cisplatin-DNA adducts and cytotoxicity. These data indicated that GOLPH3 knockdown not only enhances the pro-apoptotic effect of cisplatin, but may also elevate its DNA toxicity.

GOLPH3 knockdown elevates intracellular cisplatin level. Reduced drug accumulation is a main factor involved in cisplatin resistance (14,15). To verify the hypothesis that GOLPH3 decreased intracellular concentrations of cisplatin, the present study assessed the intracellular cisplatin concentration using cisplatin-Cy5 fluorescence. As expected, GOLPH3 knockdown in A549 cells led to enhanced cisplatin-fluorescence signal accumulation (Fig. 3A). By contrast, GOLPH3 overexpression notably decreased intracellular cisplatin concentration (Fig. 3B). Intracellular drug concentrations depend on cellular

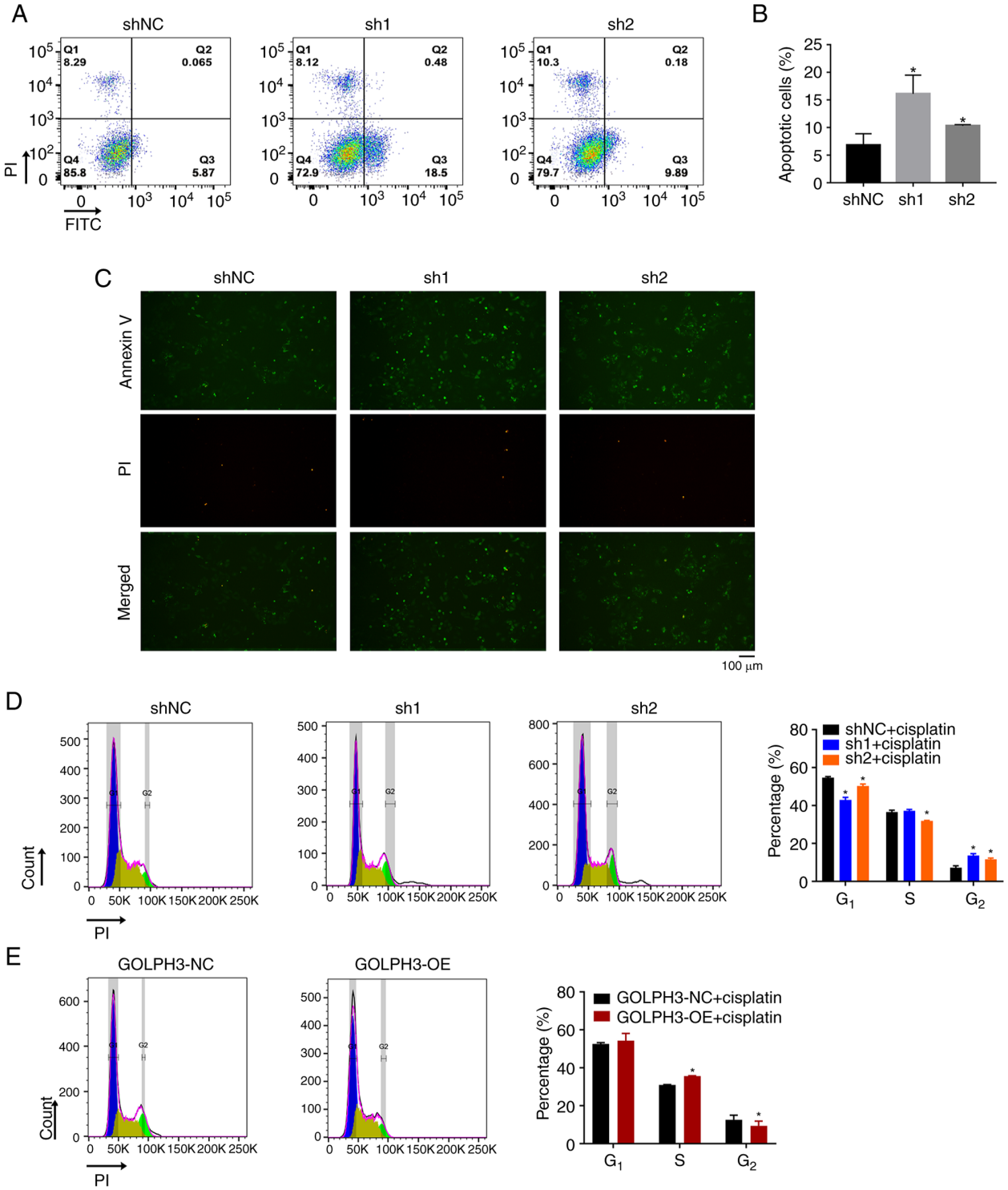

Figure 2. GOLPH3 knockdown enhances apoptosis and cell cycle arrest in A549 cells. Following treatment with 5 μg/ml cisplatin for 24 h, A549 cells infected with GOLPH3 shNC, sh1, sh2, GOLPH3-NC and GOLPH3-OE were stained with Annexin V/PI or PI for cell apoptosis or cell cycle assays, respectively. GOLPH3 knockdown increased the proportion of apoptotic cells. (A) Representative plots of flow cytometric analysis of cell apoptosis and (B) statistical analysis of the proportion of apoptotic cells. *P<0.05 vs. shNC. (C) Representative immunofluorescence images of Annexin V$^+$ and/or PI$^+$ cells. GOLPH3 knockdown prolonged the cell cycle arrest in G2 phase. (D) Representative plots of flow cytometric analysis of cell cycle progression in cells infected with shNC, sh1 and sh2 (left panel). Statistical analysis of the proportion of cells in each stage of the cell cycle (right panel). (E) Representative plots of flow cytometric analysis of cell cycle progression in cells infected with GOLPH3-NC and GOLPH3-OE cells (left panel). Statistical analysis of the proportion of cells in each stage of the cell cycle (right panel). Data are presented as the mean ± SD (n=3). GOLPH3, Golgi phosphoprotein 3; NC, negative control; OE, overexpression; PI, propidium iodide; sh, short hairpin.

uptake or efflux, and passive drug diffusion is the main form of drug accumulation. The present study aimed to uncover the biological functions of GOLPH3 on intracellular drug efflux by examining the expression levels of drug efflux transporters. RT-qPCR showed that GOLPH3 knockdown significantly downregulated ATP7A (Fig. 3C), ABCG2 (Fig. 3D), MATE1

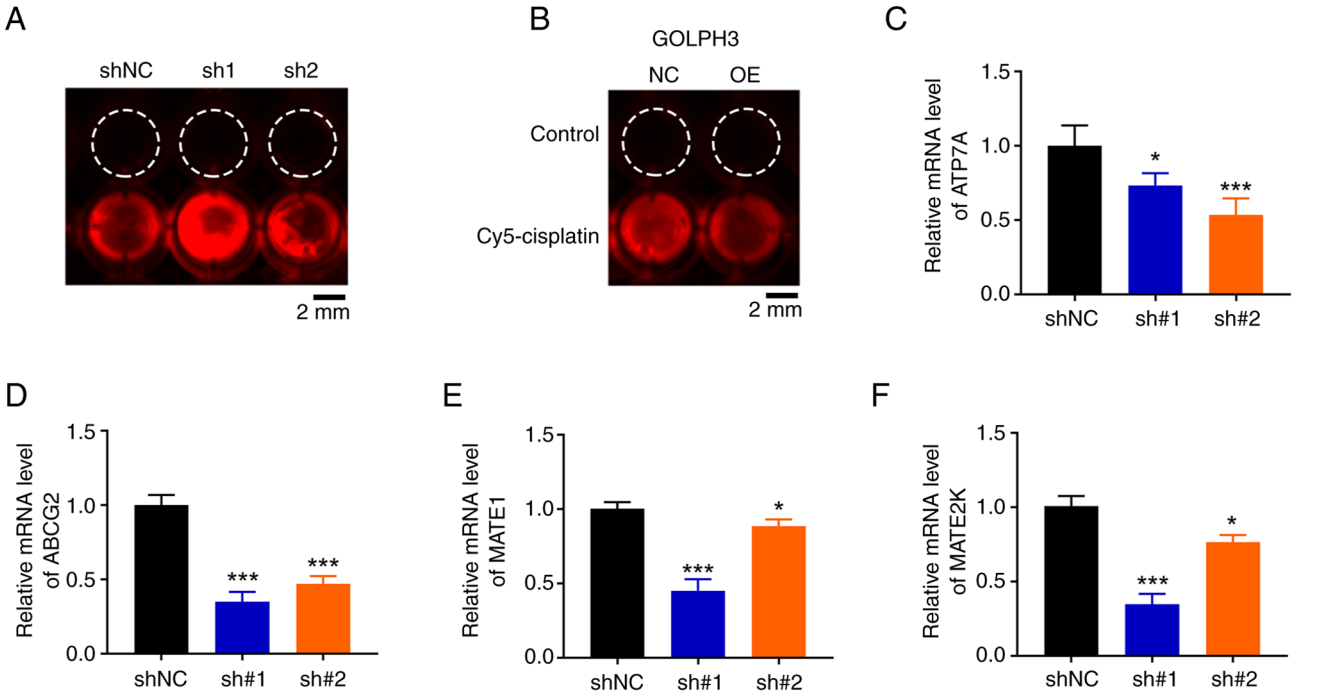

Figure 3. GOLPH3 knockdown increases cisplatin accumulation in A549 cells. A549 cells infected with (A) GOLPH3 shNC, sh1 or sh2, and (B) GOLPH3-NC or GOLPH3-OE were treated with 5 μg/ml cisplatin-Cy5 for 24 h and intracellular cisplatin-Cy5 concentration was assessed by fluorescence microscopy. Representative fluorescence images of intracellular cisplatin-Cy5 accumulation are shown. mRNA expression levels of ABC transporters, including (C) ATP7A, (D) ABCG2, (E) MATE1 and (F) MATE2K were examined relative to levels in GOLPH3-shNC cells by reverse transcription-quantitative PCR. β-actin was used as an endogenous control. Data are presented as the mean ± SD (n=3). *P<0.05, ***P<0.001 vs. shNC. GOLPH3, Golgi phosphoprotein 3; NC, negative control; OE, overexpression; PI, propidium iodide; sh, short hairpin.

(Fig. 3E) and MATE2K (Fig. 3F) mRNA expression levels compared with those in the shNC group, indicating that GOLPH3 knockdown may increase cisplatin sensitivity by downregulating the expression of ABC transporters and decreasing drug efflux.

GOLPH3 impairs glutathione (GSH)/ROS balance. Antioxidant ability assists in the survival of tumor cells treated with chemotherapy (22); therefore, the present study assessed whether GOLPH3 was associated with redox homeostasis. The levels of GSH were examined in cells with GOLPH3 knockdown or overexpression under 5 μg/ml cisplatin treatment. As shown in Fig. 4A, cells with GOLPH3 knockdown exhibited a reduction in GSH levels compared with in the control cells. By contrast, GOLPH3-overexpressing cells displayed higher levels of GSH compared with in the control cells (Fig. 4B), indicating that GOLPH3 could impair redox homeostasis by maintaining a reduced state. Notably, A549-Cis cells exhibited higher levels of GSH compared with A549 cells, which is consistent with the results of GOLPH3-overexpressing cells (Fig. S4). The present study further assessed the dependence of ROS accumulation on GOLPH3 expression. Enhanced ROS accumulation was detected in cells with GOLPH3 knockdown compared with in the control cells, whereas no notable ROS signal was detected in GOLPH3-overexpressing cells, following treatment with 5 μg/ml cisplatin (Fig. 4C). These data strongly indicated that cisplatin-mediated oxidative stress depends on cellular GOLPH3 expression, and that GOLPH3 overexpression may disrupt the GSH/ROS balance and result in cisplatin resistance.

Cisplatin resistance is associated with GOLPH3-mediated stem cell-like phenotype. Tumor stem cell subpopulations are closely associated with chemotherapeutic resistance. Therefore, the present study explored the possibility that intrinsic cisplatin resistance in NSCLC cells is due to the existence of a GOLPH3-mediated stem cell subpopulation. Cancer stem cells (CSCs) are a subpopulation of cancer cells with the ability to self-renew and drive tumorigenesis (23). As expected, the mRNA expression levels of CSC, markers (ALDH1A1, C-myc) were significantly inhibited in NSCLC cells with GOLPH3 knockdown (Fig. 5A). Tumor sphere formation assay further verified this phenomenon. The size and number of sphere colonies were markedly inhibited in cells with GOLPH3 knockdown compared with in the control group (Fig. 5B). These data suggested that GOLPH3 knockdown could suppress the stem cell-like phenotype of NSCLC cells and further elevate cisplatin sensitivity.

Discussion

The heterogeneity of NSCLC results in the short-lived potential of targeted therapy and immunotherapy. Cisplatin-based chemotherapy is of benefit for postoperative patients with NSCLC (13); however, intrinsic and acquired therapeutic resistance severely limits its clinical use (22). In addition, the molecular mechanism of cisplatin resistance in NSCLC remains unknown. The present study demonstrated the relevance of GOLPH3 protein in cisplatin resistance; knockdown of GOLPH3 markedly augmented cisplatin sensitivity. This may be attributed to the fact that low levels of GOLPH3 could

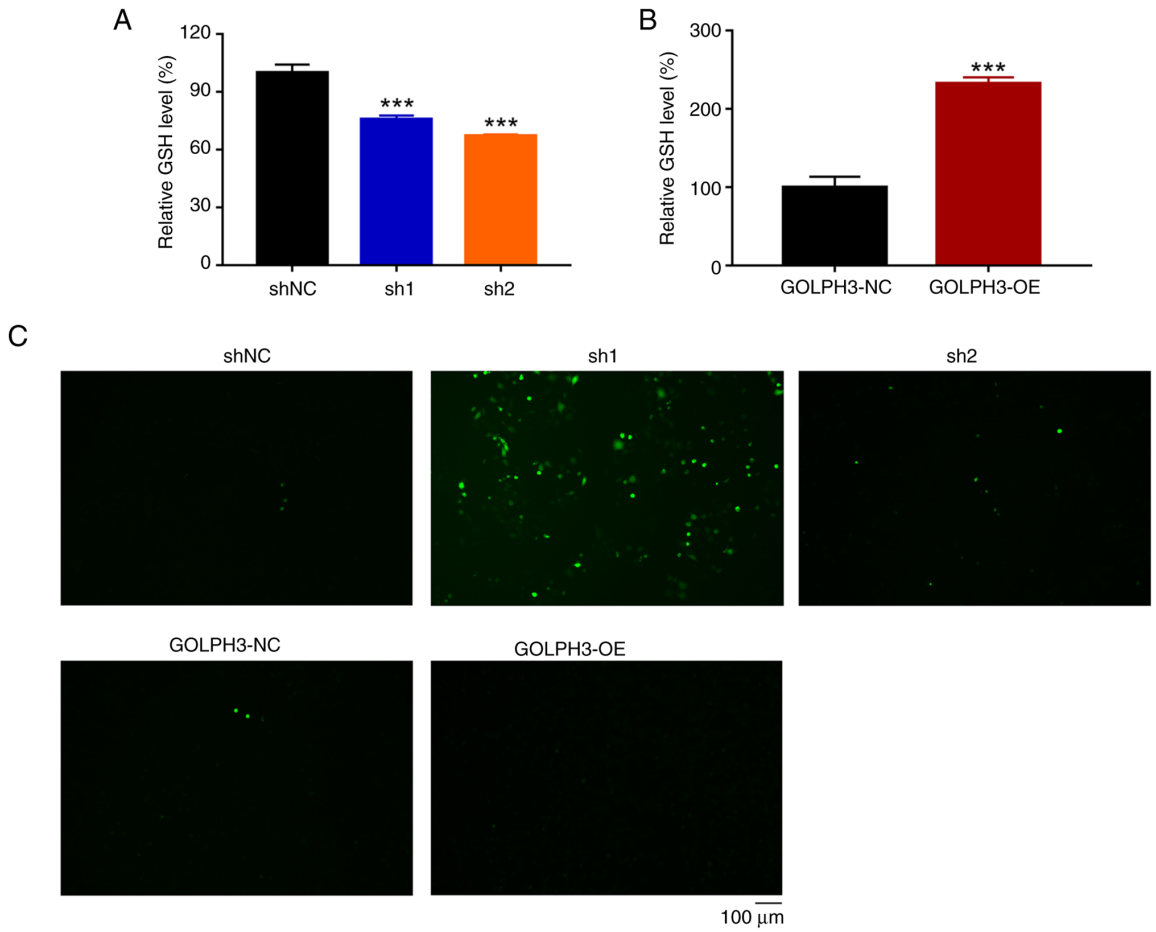

Figure 4. GOLPH3 knockdown impairs the antioxidant capacity of A549 cells. A549 cells infected with GOLPH3 shNC, sh1, sh2, GOLPH3-NC and GOLPH3-OE were treated with 5 μg/ml cisplatin for 24 h and intracellular GSH and ROS level were examined. Relative GSH level in cells infected with (A) shNC, sh1 or sh2, and (B) GOLPH3-NC or GOLPH3-OE. Data are presented as the mean ± SD (n=3). ***P<0.001 vs. shNC. (C) Cisplatin-induced ROS levels were elevated in cells with GOLPH3 knockdown, as examined using a DCFH-DA probe. Green fluorescence indicates ROS levels. GOLPH3, Golgi phosphoprotein 3; GSH, glutathione; NC, negative control; OE, overexpression; PI, propidium iodide; ROS, reactive oxygen species; sh, short hairpin.

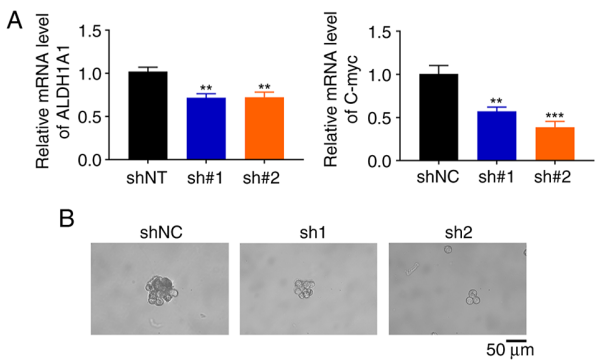

Figure 5. GOLPH3 knockdown inhibits the stem cell-like phenotype of A549 cells. (A) mRNA expression levels of stem cell markers (ALDH1A1 and C-myc) were examined relative to levels in GOLPH3-shNC cells by reverse transcription-quantitative PCR. Data are presented as the mean ± SD (n=3). **P<0.01, ***P<0.001 vs. shNC. (B) Tumor sphere formation capacity of A549 cells infected with GOLPH3 shNC, sh1 and sh2 was examined. Representative phase-contrast images of spheres formation are shown. GOLPH3, Golgi phosphoprotein 3; NC, negative control; sh, short hairpin.

inhibit the expression of ABC transporters and further mitigate cisplatin efflux. Furthermore, knockdown of GOLPH3 impaired the antioxidant ability of NSCLC cells and elevated cisplatin-associated oxidative stress. Consequently, cisplatin resistance may be attenuated by suppressing GOLPH3 protein expression.

High levels of ROS can impair tumor survival and growth; however, most tumors possess marked antioxidant capacity and thus exhibit therapeutic resistance (24,25). In NSCLC, high levels of antioxidant enzymes, such as superoxide dismutase 1 and GSH S-transferase, are commonly present in tumor tissues, and inhibition of these enzymes can increase chemotherapy-associated cell death, even in the presence of KRAS mutations that promote continued proliferation of tumor cells (26). Therefore, elevated oxidative stress may be a novel avenue for cancer therapy. The present study demonstrated a novel biological function of GOLPH3 that is relevant to cellular redox balance. Knockdown of GOLPH3 significantly reduced intracellular GSH levels, which is a key antioxidant that could bind to cisplatin to form a deactivated complex readily excreted by a GSH S-conjugated export pump, resulting in enhanced drug accumulation and increased drug sensitivity. By contrast, knockdown of GOLPH3 elevated intracellular ROS levels. As high levels of GSH are often associated with cisplatin resistance and tumor malignancy, elucidating the relevance of GOLPH3 and GSH/ROS balance may expand clinical application and overcome cisplatin resistance.

CSCs are a small heterogeneous subpopulation of tumor cells that not only maintain the renewal capability of tumor cells, but are also related to the resistance of tumor cells to chemotherapy or radiotherapy (27). Since increasing studies have reported that the PI3K-Akt-mTOR signaling pathway is the major regulator of CSCs, which is involved in the maintenance of stemness, proliferation, differentiation and survival, inhibition of mTOR pathway activity may be a promising therapeutic strategy for CSC-associated drug resistance (28,29). Notably, GOLPH3, a Golgi oncoprotein, is an inherent initiator of the activation of mTOR and its downstream signaling (17). The present study revealed that knockdown of GOLPH3 markedly inhibited the expression levels of the CSC markers ALDH1A and C-myc in NSCLC cells. Consistent with these results, fewer tumor spheres were formed in cells with GOLPH3 knockdown than in control cells.

It is important to acknowledge that the absence of another NSCLC cell line, primary NSCLC cells or an animal model in the present study represents a potential limitation. The lack of additional models restricts the generalizability and clinical relevance of the findings; therefore, future investigations should consider incorporating these supplementary models to provide a more comprehensive evaluation of the therapeutic potential of GOLPH3 inhibition.

In summary, the present study revealed the relevance of GOLPH3 in cisplatin resistance in the A549 NSCLC cell line. Knockdown of GOLPH3 not only increased cisplatin accumulation but also elevated oxidative stress in these cells. In addition, knockdown of GOLPH3 diminished the CSC-like properties of NSCLC cells and restored cisplatin sensitivity. Thus, inhibition of GOLPH3 may be considered a promising therapeutic strategy for cisplatin resistance in NSCLC. These findings should be further investigated *in vivo* and in the clinic to determine whether inhibition of GOLPH3 could be translated from experimental research to clinical application.

Acknowledgements

Not applicable.

Funding

This work was supported by the Education and Research Project for Middle and Young Teachers in Fujian Province (Science and Technology), China (grant no. JAT210124); the Startup Fund for Scientific Research, Fujian Medical University, China (grant no. 2021QH1024); and Fujian Provincial Natural Science Foundation of China (grant no. 2023J01635).

Availability of data and materials

The data generated in the present study may be requested from the corresponding author.

Authors' contributions

DX conceived and designed the experiments. QW, ZL and JL performed the experiments. QW, ZL, NY, YW, XT and JL performed the data analyses. QW, ZL and JL drafted and revised the manuscript. DX finalized the manuscript. QW and DX confirm the authenticity of all the raw data. All authors read and approved the final version of the manuscript.

Ethics approval and consent to participate

Not applicable.

Patient consent for publication

Not applicable.

Competing interests

The authors declare that they have no competing interests.

References

1. Siegel RL, Miller KD, Wagle NS and Jemal A: Cancer statistics, 2023. CA Cancer J Clin 73: 17-48, 2023.
2. Torre LA, Siegel RL and Jemal A: Lung cancer statistics. Adv Exp Med Biol 893: 1-19, 2016.
3. Miller KD, Nogueira L, Devasia T, Mariotto AB, Yabroff KR, Jemal A, Kramer J and Siegel RL: Cancer treatment and survivorship statistics, 2022. CA Cancer J Clin 72: 409-436, 2022.
4. Wang M, Herbst RS and Boshoff C: Toward personalized treatment approaches for non-small-cell lung cancer. Nat Med 27: 1345-1356, 2021.
5. Banfill K, Giuliani M, Aznar M, Franks K, McWilliam A, Schmitt M, Sun F, Vozenin MC, Faivre Finn C and IASLC Advanced Radiation Technology committee: Cardiac toxicity of thoracic radiotherapy: Existing evidence and future directions. J Thorac Oncol 16: 216-227, 2021.
6. Bentzen SM: Preventing or reducing late side effects of radiation therapy: Radiobiology meets molecular pathology. Nat Rev Cancer 6: 702-713, 2006.
7. Wennerberg E, Mukherjee S, Spada S, Hung C, Agrusa CJ, Chen C, Valeta-Magara A, Rudqvist NP, Van Nest SJ, Kamel MK, *et al*: Expression of the mono-ADP-ribosyltransferase ART1 by tumor cells mediates immune resistance in non-small cell lung cancer. Sci Transl Med 14: eabe8195, 2022.
8. Horvath L, Thienpont B, Zhao L, Wolf D and Pircher A: Overcoming immunotherapy resistance in non-small cell lung cancer (NSCLC)-novel approaches and future outlook. Mol Cancer 19: 141, 2020.
9. De Ruysscher D, Faivre-Finn C, Nackaerts K, Jordan K, Arends J, Douillard JY, Ricardi U and Peters S: Recommendation for supportive care in patients receiving concurrent chemotherapy and radiotherapy for lung cancer. Ann Oncol 31: 41-49, 2020.
10. Rinaldi M, Cauchi C and Gridelli C: First line chemotherapy in advanced or metastatic NSCLC. Ann Oncol 17 (Suppl 5): v64-v67, 2006.
11. Tsan DL, Lin CY, Kang CJ, Huang SF, Fan KH, Liao CT, Chen IH, Lee LY, Wang HM and Chang JT: The comparison between weekly and three-weekly cisplatin delivered concurrently with radiotherapy for patients with postoperative high-risk squamous cell carcinoma of the oral cavity. Radiat Oncol 7: 215, 2012.
12. Chaft JE, Rimner A, Weder W, Azzoli CG, Kris MG and Cascone T: Evolution of systemic therapy for stages I-III non-metastatic non-small-cell lung cancer. Nat Rev Clin Oncol 18: 547-557, 2021.
13. Pignon JP, Tribodet H, Scagliotti GV, Douillard JY, Shepherd FA, Stephens RJ, Dunant A, Torri V, Rosell R, Seymour L, *et al*: Lung adjuvant cisplatin evaluation: A pooled analysis by the LACE collaborative group. J Clin Oncol 26: 3552-3559, 2008.
14. Sun Y, Shen W, Hu S, Lyu Q, Wang Q, Wei T, Zhu W and Zhang J: METTL3 promotes chemoresistance in small cell lung cancer by inducing mitophagy. J Exp Clin Cancer Res 42: 65, 2023.
15. Wang D, Zhao C, Xu F, Zhang A, Jin M, Zhang K, Liu L, Hua Q, Zhao J, Liu J, *et al*: Cisplatin-resistant NSCLC cells induced by hypoxia transmit resistance to sensitive cells through exosomal PKM2. Theranostics. 11: 2860-2875, 2021.

16. Song JW, Zhu J, Wu XX, Tu T, Huang JQ, Chen GZ, Liang LY, Zhou CH, Xu X and Gong LY: GOLPH3/CKAP4 promotes metastasis and tumorigenicity by enhancing the secretion of exosomal WNT3A in non-small-cell lung cancer. Cell Death Dis 12: 976, 2021.
17. Scott KL, Kabbarah O, Liang MC, Ivanova E, Anagnostou V, Wu J, Dhakal S, Wu M, Chen S, Feinberg T, *et al*: GOLPH3 modulates mTOR signalling and rapamycin sensitivity in cancer. Nature 459: 1085-1090, 2009.
18. Yu T, An Q, Cao XL, Yang H, Cui J, Li ZJ and Xiao G: GOLPH3 inhibition reverses oxaliplatin resistance of colon cancer cells via suppression of PI3K/AKT/mTOR pathway. Life Sci 260: 118294, 2020.
19. Wang MZ, Qiu CZ, Yu WS, Guo YT, Wang CX and Chen ZX: GOLPH3 expression promotes the resistance of HT29 cells to 5-fluorouracil by activating multiple signaling pathways. Mol Med Rep 17: 542-548, 2018.
20. Gao Y, Yin Z, Qi Y, Peng H, Ma W, Wang R and Li W: Golgi phosphoprotein 3 promotes angiogenesis and sorafenib resistance in hepatocellular carcinoma via upregulating exosomal miR-494-3p. Cancer Cell Int 22: 35, 2022.
21. Livak KJ and Schmittgen TD: Analysis of relative gene expression data using real-time quantitative PCR and the 2(-Delta Delta C(T)) Method. Methods 25: 402-408, 2001.
22. Meng F, Li Y, Liu Q, Sun L, Wang H, Li X, Li G and Chen F: Experimental study of camptothecin combined with drug-eluting bead transarterial chemoembolization in the rabbit VX2 liver tumor model. Front Oncol 12: 906971, 2022.
23. Qi Y, Wei J and Zhang X: Requirement of transcription factor NME2 for the maintenance of the stemness of gastric cancer stem-like cells. Cell Death Dis 12: 924, 2021.
24. Fuertes MA, Alonso C and Pérez JM: Biochemical modulation of Cisplatin mechanisms of action: Enhancement of antitumor activity and circumvention of drug resistance. Chem Rev 103: 645-662, 2003.
25. Zalewska-Ziob M, Adamek B, Kasperczyk J, Romuk E, Hudziec E, Chwalińska E, Dobija-Kubica K, Rogoziński P and Bruliński K: Activity of antioxidant enzymes in the tumor and adjacent noncancerous tissues of non-small-cell lung cancer. Oxid Med Cell Longev 2019: 2901840, 2019.
26. Wu C, Liu Z, Chen Z, Xu D, Chen L, Lin H and Shi J: A nonferrous ferroptosis-like strategy for antioxidant inhibition-synergized nanocatalytic tumor therapeutics. Sci Adv 7: eabj8833, 2021.
27. Glasauer A, Sena LA, Diebold LP, Mazar AP and Chandel NS: Targeting SOD1 reduces experimental non-small-cell lung cancer. J Clin Invest 124: 117-128, 2014.
28. Karami Fath M, Ebrahimi M, Nourbakhsh E, Zia Hazara A, Mirzaei A, Shafieyari S, Salehi A, Hoseinzadeh M, Payandeh Z and Barati G: PI3K/Akt/mTOR signaling pathway in cancer stem cells. Pathol Res Pract 237: 154010, 2022.
29. Yang L, Shi P, Zhao G, Xu J, Peng W, Zhang J, Zhang G, Wang X, Dong Z, Chen F and Cui H: Targeting cancer stem cell pathways for cancer therapy. Signal Transduct Target Ther 5: 8, 2020.